

# Comparison of Denitrification Activity Measurements in Groundwater Using Cores and Natural-Gradient Tracer Tests

RICHARD L. SMITH\*

*U.S. Geological Survey, 3215 Marine Street,  
Boulder, Colorado 80303*

STEPHEN P. GARABEDIAN

*U.S. Geological Survey, 28 Lord Street,  
Marlborough, Massachusetts 01752*

MYRON H. BROOKS

*U.S. Geological Survey, 3215 Marine Street,  
Boulder, Colorado 80303*

The transport of many solutes in groundwater is dependent upon the relative rates of physical flow and microbial metabolism. Quantifying rates of microbial processes under subsurface conditions is difficult and is most commonly approximated using laboratory studies with aquifer materials. In this study, we measured in situ rates of denitrification in a nitrate-contaminated aquifer using small-scale, natural-gradient tracer tests and compared the results with rates obtained from laboratory incubations with aquifer core material. Activity was measured using the acetylene block technique. For the tracer tests, co-injection of acetylene and bromide into the aquifer produced a 30  $\mu\text{M}$  increase in nitrous oxide after 10 m of transport (23–30 days). An advection–dispersion transport model was modified to include an acetylene-dependent nitrous oxide production term and used to simulate the tracer breakthrough curves. The model required a 4-day lag period and a relatively low sensitivity to acetylene to match the narrow nitrous oxide breakthrough curves. Estimates of in situ denitrification rates were 0.60 and 1.51  $\text{nmol}$  of  $\text{N}_2\text{O}$  produced  $\text{cm}^{-3}$  aquifer  $\text{day}^{-1}$  for two successive tests. Aquifer core material collected from the tracer test site and incubated as mixed slurries in flasks and as intact cores yielded rates that were 1.2–26 times higher than the tracer test rate estimates. Results with the coring-dependent techniques were variable and subject to the small-scale heterogeneity within the aquifer, while the tracer tests integrated the heterogeneity along a flow path, giving a rate estimate that is more applicable to transport at the scale of the aquifer.

## Introduction

Microorganisms are key factors that control the chemistry of groundwater. Microbial populations can have profound effects upon the transport and fate of both naturally-occurring and contaminant solutes (1, 2). Therefore, to fully understand the geochemistry of groundwater, it is important to be able to determine the extent to which and the rates at which microbial processes are occurring in the subsurface and to do so within the context of the hydrologic regime. However, this has proven to be a difficult task.

In general, except for heavily contaminated situations, groundwater microbial processes proceed at rates that are slower than the rate of groundwater flow; that is, many solutes are transported faster than they are transformed. This is due to the nutrient- and energy-poor nature of the groundwater environment. This fact, which necessitates long-term incubations, coupled with the difficulty in obtaining undisturbed and uncompromised core samples from the subsurface, makes it difficult to assess whether rate measurements of microbial processes that are determined in the laboratory with aquifer materials are relevant to actual in situ rates (3, 4). Natural-gradient tracer tests offer an alternative approach in which microbial processes can be measured directly within an aquifer (5, 6). These tests utilize the transport of tracers through an undisturbed portion of an aquifer by natural groundwater flow. Thus, microbial processes can be examined with minimal alteration of their native environment, and the resulting rate measurements are more likely to be reasonable estimates of in situ activity.

In this study, we compared the results of laboratory incubations using aquifer core material with those determined using natural gradient tracer tests to estimate the in situ rate of a microbial process in groundwater. Denitrification was chosen as the subject process because (1) nitrate is one of the most prevalent contaminants in groundwater; (2) as a terminal electron-accepting process, whenever it occurs in groundwater, denitrification is the focal point of energy flow through the entire microbial food chain; and (3) the acetylene block technique provided a sufficiently sensitive assay to measure the relatively slow rates at which the process occurs in most groundwaters. We found that both whole core and sediment slurry incubations overestimated the rate of denitrification as compared to the in situ natural-gradient tracer tests. The tracer tests also integrated the heterogeneity that occurred along a flow path within an aquifer and so, in general, gave results that were more pertinent to the scale of an aquifer.

## Experimental Section

**Study Site.** This study was conducted in a freshwater sand and gravel aquifer located on Cape Cod near Falmouth, MA (Figure 1A). At this location, disposal of dilute, treated sewage has resulted in a large plume of contaminated groundwater (4 km long), which has been the focus of several previous studies on contaminant transport in groundwater (7–13). Nitrate and ammonium are signifi-

\* Corresponding author: telephone: 303-541-3032; fax: 303-447-2505; e-mail address: rlsmith@usgs.gov.

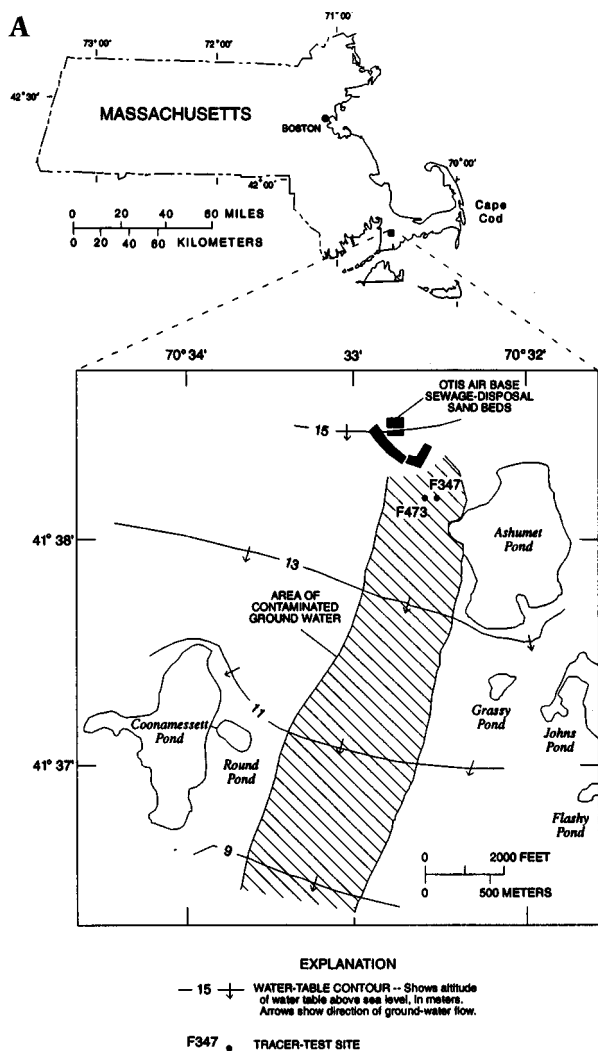


FIGURE 1. Groundwater study site on Cape Cod, MA, showing (A) the location of the contaminant plume, the source of the plume, and two of the well sites used to study denitrification and (B) the tracer test array at site F473.

cant components of the contaminant plume (8, 14), often exceeding concentrations of 1 mM. Dissolved organic carbon in the plume is 2–4 mg/L, but is composed of mostly refractory compounds (15, 16). Because much of the contaminated groundwater is suboxic or anoxic, denitrification is one of the predominant terminal electron-accepting processes in the plume, and it is a key factor in carbon and nitrogen cycling by microorganisms within the affected portions of the aquifer (14, 17). However, dissi-

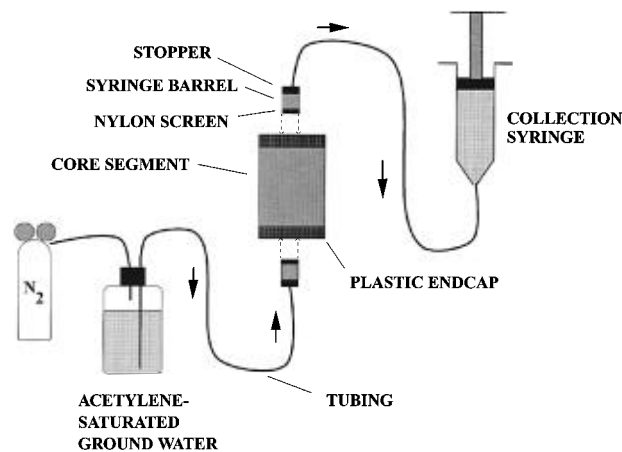


FIGURE 2. Diagram of the apparatus used to replace and collect the interstitial porewater from sediment cores.

military reduction of nitrate to ammonium is not significant (14, 17). For this study, sediment and groundwater were collected from site F473, which is located about 2 years groundwater travel time from the contaminant source (Figure 1). This site and nearby site F347 were the locations for previous studies on denitrification in ground water (14, 17–19).

**Incubations with Aquifer Sediments.** Groundwater was pumped from multilevel samplers (11) into 1-L glass bottles as described by Brooks et al. (18) and stored at 4 °C. Aquifer sediments were collected with a wire-line piston core barrel through hollow stem augers (20). The core barrel was fitted with a 5.1 cm diameter, 1.5 m long aluminum liner, which was cut into 0.3-m segments upon retrieval. Each segment was then capped and stored at 4 °C. All incubations were begun within 24 h of collection of the groundwater and sediment samples.

Denitrifying activity was assayed in both sediment slurry incubations and whole core incubations using the acetylene blockage technique (21). For sediment slurry incubations, aquifer sediment was extruded in an anaerobic glovebag and mixed, and 75–85 g (wet wt) was transferred to 125-mL flasks. Fifty milliliters of groundwater (obtained from the same depth and location as the core material) was added to each flask; the flasks were stoppered, sealed with vinyl tape, and flushed for 30 min with O<sub>2</sub>-free N<sub>2</sub>. The flasks were placed in a 12 °C shaking water bath for 3 h, and then 15 mL of acetylene was added to each. Gas samples were withdrawn periodically from each flask headspace and assayed for nitrous oxide.

Whole core incubations were conducted using a pore-water replacement procedure shown in Figure 2. The cap on a 1-L bottle containing groundwater was replaced with a rubber stopper connected to Tygon tubing, and 250 mL of acetylene was added through the stopper by syringe, displacing groundwater out through the tubing. Holes were cut in the endcap of a core segment with a cork bore, and the core segment was connected via tubing to the bottle containing the groundwater at one end and a collection syringe at the other end (Figure 2). The acetylene-amended water was forced through the core in an up-flow mode using line pressure from a tank of N<sub>2</sub> (~4 psi); the flow rate was 10–15 mL min<sup>-1</sup>. The porewater exiting the core, which was clear, was collected in the syringe. The first 200 mL

passing through the core was discarded; the next 30 mL was filtered and frozen for nitrate analysis. The last two 15-mL aliquots were injected into stoppered 30-mL serum bottles and assayed for the zero time nitrous oxide concentration. The cores were then disconnected from the tubing, the holes in the endcap were plugged with solid rubber stoppers, and the cores were placed in a 12 °C water bath for 8 days. At the end of the incubation, the cores were reconnected to the porewater displacement train. In this case, porewater was displaced with distilled water containing a blue dye and collected in 15 mL aliquots (usually 7–9) until the blue color was visually evident. Each aliquot was injected into a stoppered 30-mL serum bottle and assayed for nitrous oxide concentration. The content of each core was then extruded, dried, and weighed.

**Tracer Tests.** Natural-gradient tracer tests were conducted as previously described (5). Briefly, an injection solution was prepared by pumping 100 L of groundwater from an injection well multilevel sampler (MLS) (Figure 1B) with a peristaltic pump into a gas-impermeable bladder. Prior to filling, the bladder had been sparged 7 times with N<sub>2</sub>, deflated, and loaded with an anoxic solution (1 L, 125 mM) of NaBr. After filling the bladder with groundwater, acetylene (5–10 L) was added and equilibrated with the groundwater for 1–2 h with frequent mixing, and then any undissolved gas was vented. The injectate solution was then pumped into the aquifer through the injection well; samples were collected during the beginning, middle, and end of the injection process and analyzed for bromide, acetylene, oxygen, nitrate, and nitrite. During the entire procedure, the bladder was kept in a large plastic-lined pit filled with groundwater to minimize temperature changes.

The tracer cloud moved downgradient with natural groundwater flow. It was intercepted and sampled at a row of 15-port MLSs (spaced 1.1 m apart perpendicular to groundwater flow) 10.0 m from the injection well (Figure 1B). Water samples were collected daily from the sampling grid with a peristaltic pump. Samples to be analyzed for (1) nitrate and nitrite were filtered (0.45 μm) and frozen; (2) nitrous oxide and acetylene were collected in a syringe (15 mL) and injected into stoppered 30-mL serum bottles that contained 200 μL of 12.5 N NaOH; and (3) bromide were collected in plastic 60-mL bottles.

**Model Formulation.** A numerical solution of the advection–dispersion equation was used to simulate the movement and spreading of bromide and acetylene and, with the addition of a zero-order reaction term, the production of nitrous oxide in the small-scale injection tests. The derivation of this equation is based on several assumptions, including a constant groundwater velocity and a constant dispersion coefficient (i.e., dispersion of the solutes follows Fick's law). The one-dimensional transport equation, which contains terms for storage, dispersion, advection, and zero-order production, can be written as

$$\frac{\partial c}{\partial t} = D \frac{\partial^2 c}{\partial x^2} - v \frac{\partial c}{\partial x} + \frac{k}{n} \quad (1)$$

where  $c$  is the concentration of the solute,  $t$  is time,  $x$  is the spatial coordinate in the direction of flow,  $D$  is the dispersion coefficient (equal to  $\alpha_L v$ ),  $\alpha_L$  is the dispersivity,  $v$  is the fluid velocity,  $k$  is the zero-order production rate, and  $n$  is the aquifer porosity. Because  $k$  is dependent on the concen-

tration of acetylene ( $2I$ ), the linkage between  $k$  and acetylene concentrations was modeled using

$$k = 0 \quad A \leq A_{\min} \quad (2a)$$

$$k = k_{\max} \left( \frac{A - A_{\min}}{A_{\max} - A_{\min}} \right) \quad A_{\min} \leq A \leq A_{\max} \quad (2b)$$

$$k = k_{\max} \quad A \geq A_{\max} \quad (2c)$$

where  $A$  is the simulated concentration of acetylene,  $A_{\min}$  is the threshold acetylene concentration at which the block begins to be effective in preventing reduction of nitrous oxide, and  $A_{\max}$  is the acetylene concentration at which the maximum nitrous oxide production rate ( $k_{\max}$ ) is reached.

The modeling approach used in this study to simulate the production and transport of nitrous oxide was to first compute the physical transport parameter values ( $v$ ,  $\alpha_L$ ) by calibrating numerical model solutions to the observed breakthrough curves of the nonreactive tracer (bromide), then use these parameter values to simulate the transport of acetylene, and finally estimate the nitrous oxide production parameter ( $k_{\max}$ ) by calibrating numerical solutions of eq 1 to observed nitrous oxide breakthrough curves. For the transport of bromide, the production rate ( $k_{\max}$ ) is set to zero, and the fluid velocity ( $v$ ) is calculated from the known distance between the injection and sampling point ( $x_1$ ) and the time to the peak concentration ( $t_{\text{peak}}$ ) for the breakthrough curve ( $v = x_1/t_{\text{peak}}$ ). The dispersivity parameter ( $\alpha_L$ ) is obtained from the bromide curve using the following relation, derived from the one-dimensional solution of the advection–dispersion equation with a pulse input:

$$\alpha_L = \frac{x^2 (\Delta t / t_{\text{peak}})^2}{16 \ln(2)} \quad (3)$$

where  $\Delta t$  is the duration of the breakthrough curve when  $\text{Br} > 0.5 \text{ Br}_{\max}$ ,  $\text{Br}_{\max}$  is the peak concentration, and  $t_{\text{peak}}$  is the time to peak concentration.

The numerical model was developed by solving eq 1 using finite difference approximations with a Crank–Nicholson time-stepping scheme (22). After the approximations are introduced, eq 1 is reduced to an algebraic form:

$$c(x - \Delta x, t + \Delta t) \left\{ \frac{-D}{2(\Delta x)^2} + \frac{-v}{4(\Delta x)} \right\} + c(x, t + \Delta t) \times \left\{ \frac{1}{\Delta t} + \frac{D}{(\Delta x)^2} \right\} + c(x + \Delta x, t + \Delta t) \left\{ \frac{-D}{2(\Delta x)^2} + \frac{v}{4(\Delta x)} \right\} = c(x - \Delta x, t) \left\{ \frac{D}{2(\Delta x)^2} + \frac{v}{4(\Delta x)} \right\} + c(x, t) \times \left\{ \frac{1}{\Delta t} + \frac{-D}{(\Delta x)^2} \right\} + c(x + \Delta x, t) \left\{ \frac{D}{2(\Delta x)^2} + \frac{-v}{4(\Delta x)} \right\} + \frac{k}{n} \quad (4)$$

where  $\Delta x$  is the block size (0.01 m) and  $\Delta t$  is the time step (0.02 day). All of the concentration values on the left-hand side [ $c(x - \Delta x, t + \Delta t)$ ,  $c(x, t + \Delta t)$ ,  $c(x + \Delta x, t + \Delta t)$ ] are at the new time step ( $t + \Delta t$ ) and are unknown; those on the right-hand side [ $c(x - \Delta x, t)$ ,  $c(x, t)$ ,  $c(x + \Delta x, t)$ ] are at the present level and are known. After calculating the new concentrations for all blocks within the domain, these values are then used as the present level, and another set is calculated for the next time step, marching onward in time. Because of the form of eq 4, a tridiagonal matrix solution

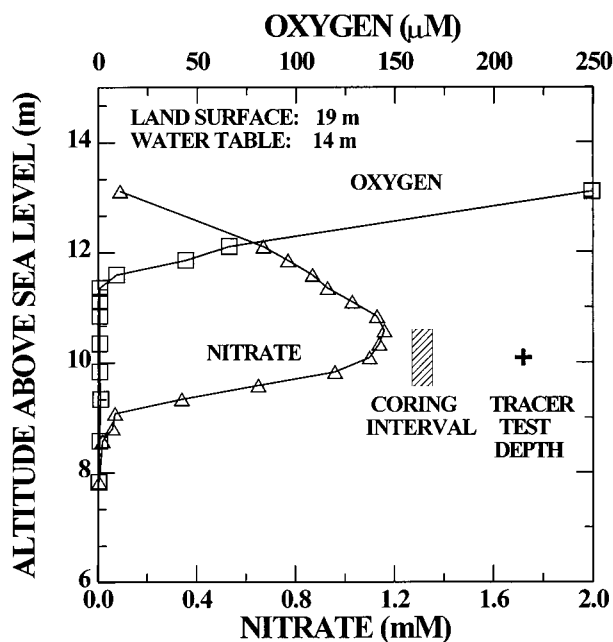


FIGURE 3. Vertical profile of dissolved oxygen and nitrate in groundwater collected from site F473 in May 1991.

is used that is both efficient and accurate. Restrictions on the grid Peclet number and the Courant number, required for numerical model stability, were calculated for these simulations, and the block size and the time step were limited to satisfy these restrictions.

**Analytical Techniques.** Nitrous oxide was measured with a gas chromatograph equipped with an electron capture detector (18). Acetylene was measured by gas chromatography using a flame ionization detector (23). Aqueous concentrations of each gas were calculated using Bunsen solubility coefficients (24, 25). Nitrate and nitrite were analyzed colorimetrically with a flow injection autoanalyzer using the cadmium reduction technique (26). Oxygen was determined with both an oxygen-specific probe and colorimetrically (10), while bromide was measured in the field with an ion-specific electrode, and the results were corroborated using a colorimetric assay with a flow injection autoanalyzer (27).

## Results and Discussion

Groundwater chemistry at the study site delineated the sharp vertical gradients that are typical of this Cape Cod contaminant plume (Figure 3) (28). The shallowest groundwater was uncontaminated, containing dissolved oxygen concentrations greater than 200  $\mu\text{M}$ . Oxygen decreased rapidly with depth to very low levels within the plume. The upper portions of the contaminant plume contained nitrate, with peak concentrations exceeding 1 mM, and most of which was anoxic. Groundwater and core samples were obtained from and natural-gradient tracer tests were conducted within this nitrate-containing zone for the denitrification assays (Figure 3).

Aquifer core material that had been slurried with groundwater that was obtained from the same location and depth produced nitrous oxide when incubated in the presence of acetylene (Figure 4). Nitrous oxide production is the result of denitrifying activity within the slurried material, and its accumulation is caused by inhibition of nitrous oxide reductase, the terminal enzyme of the denitrification pathway, by the presence of the added

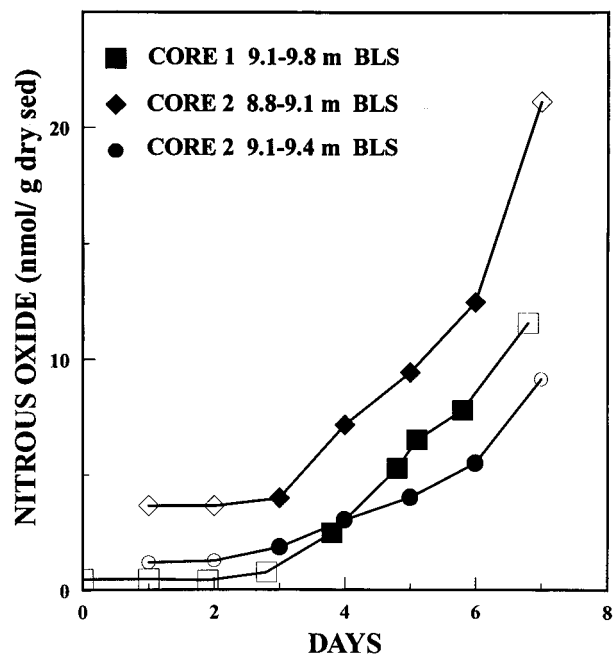


FIGURE 4. Time course of nitrous oxide production by sediment slurries incubated in the presence of acetylene. Incubations were conducted at ambient temperature ( $12^\circ\text{C}$ ) and nitrate concentration. Core 1 was collected in June 1991; points are means of quadruplicate flasks. Core 2 was collected in August 1991; points are means of triplicate flasks. Solid symbols are data points used for rate determination by linear regression (BLS = below land surface).

acetylene (21). A 3–4-day lag in nitrous oxide accumulation was evident and reproducible in different batches of core material and is characteristic of acetylene block assays with core and groundwater samples from this aquifer (17, 18). Denitrification is actively occurring in the aquifer in the region from which these samples were taken (14, 17, 18), thus the lag is not due to induction of a process that is inactive in situ. After the time lag, nitrous oxide production was linear for a period of several days (Figure 4). Rates of production were calculated using a linear regression of the time points immediately following the cessation of the lag. Differences in the rate of nitrous oxide accumulation were evident between and within cores (Figure 4). DeSimone and Howes (29) found similar results when assaying a sandy glacial aquifer for denitrification using sediment slurry incubations.

The sediment slurry incubations were conducted under near in situ conditions, using freshly-collected core and water samples while maintaining the ambient geochemical regime and ambient temperature. However, the sediment to water ratio differed greatly from the aquifer, and the core material was manipulated and shaken during the incubation. This invasive approach has the potential for increasing the availability of nutrients and organic substrates due to abrasion and desorption during the incubation. For surface water sediments, tracer techniques have been developed to conduct incubations directly within intact cores to further maintain the physical conditions of the environment (30). More recently, this technique has also been applied to aquifer cores (29). In this study, we used an analogous approach that exploits the aqueous transmissivity of the aquifer solids. Acetylene-saturated groundwater was gently forced into the aquifer cores (Figure 2) replacing the pore fluid in the core. With this approach there is minimal physical disruption during the incubation,

TABLE 1

## Nitrous Oxide Production in Intact Aquifer Cores Incubated in Presence of Acetylene

core/interval (m BLS) <sup>a</sup>	N <sub>2</sub> O in pore water (μM)		N <sub>2</sub> O production rate (nmol (g dry sed) <sup>-1</sup> day <sup>-1</sup> )
	0 days	8 days	
A 8.8–9.1	4.7	162.2	3.98
A 9.1–9.4	2.3	52.2	1.26
B 8.8–9.1	4.5	163.4	4.02
B 9.1–9.4	2.6	156.4	3.89
C 8.8–9.1	5.3	97.1	2.32
C 9.1–9.4	1.8	95.6	2.37

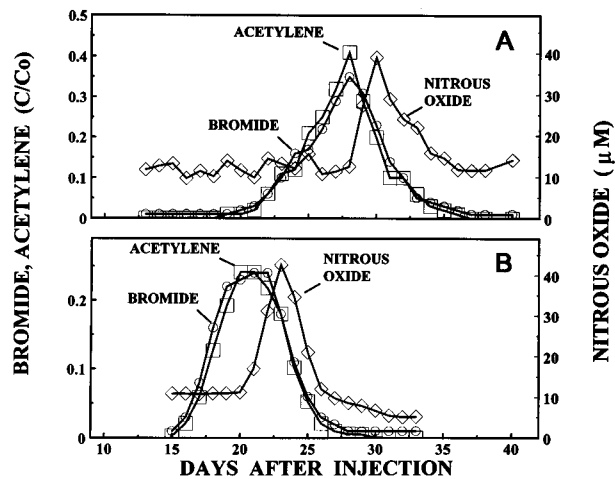
<sup>a</sup> BLS, below land surface.

FIGURE 5. Time course of the relative concentrations of acetylene and bromide tracers and the resulting production of nitrous oxide in groundwater for natural-gradient tracer tests conducted in (A) 1992 and (B) 1991. The data are for water samples collected from two different multilevel samplers (one for each year) that were located in a row of multilevel samplers 10.0 m downgradient from the injection well.

the porosity of the core is preserved, and the chemistry of the pore fluid mimics in situ conditions.

There was a significant increase in porewater nitrous oxide concentrations within the intact cores after an 8-day incubation (Table 1). Mean values of the aliquots of displaced pore water varied 9–38% (SD) within a core segment. Overall, the rates of nitrous oxide production in the intact core incubations varied ~3-fold, from 1.26–4.02 nmol N<sub>2</sub>O (g dry sediment)<sup>-1</sup> day<sup>-1</sup> in the depth interval 8.8–9.4 m below land surface (10.2–9.6 m altitude) (Table 1). These denitrification rates are probably zero order with respect to the high nitrate concentrations in the porewater of the cores (0.3–0.9 mM). It is unknown whether a time lag occurred at the onset of the incubation in the intact cores. Rates of activity were calculated assuming constant production of nitrous oxide over the whole incubation period. Time course incubations with sequential sacrifice of replicate cores were not conducted due to prohibitive drilling costs.

It is difficult to reproduce the physical environment of an aquifer in the laboratory. Conducting activity assays directly in the aquifer within the natural hydraulic gradient eliminates the need to do so and quantifies microbial processes with minimal disturbance. Therefore, denitrifying activity at the Cape Cod field site was assessed directly within the aquifer using natural-gradient tracer tests with acetylene. Nitrous oxide was produced within the tracer cloud in the nitrate-containing zone (see Figure 3); an

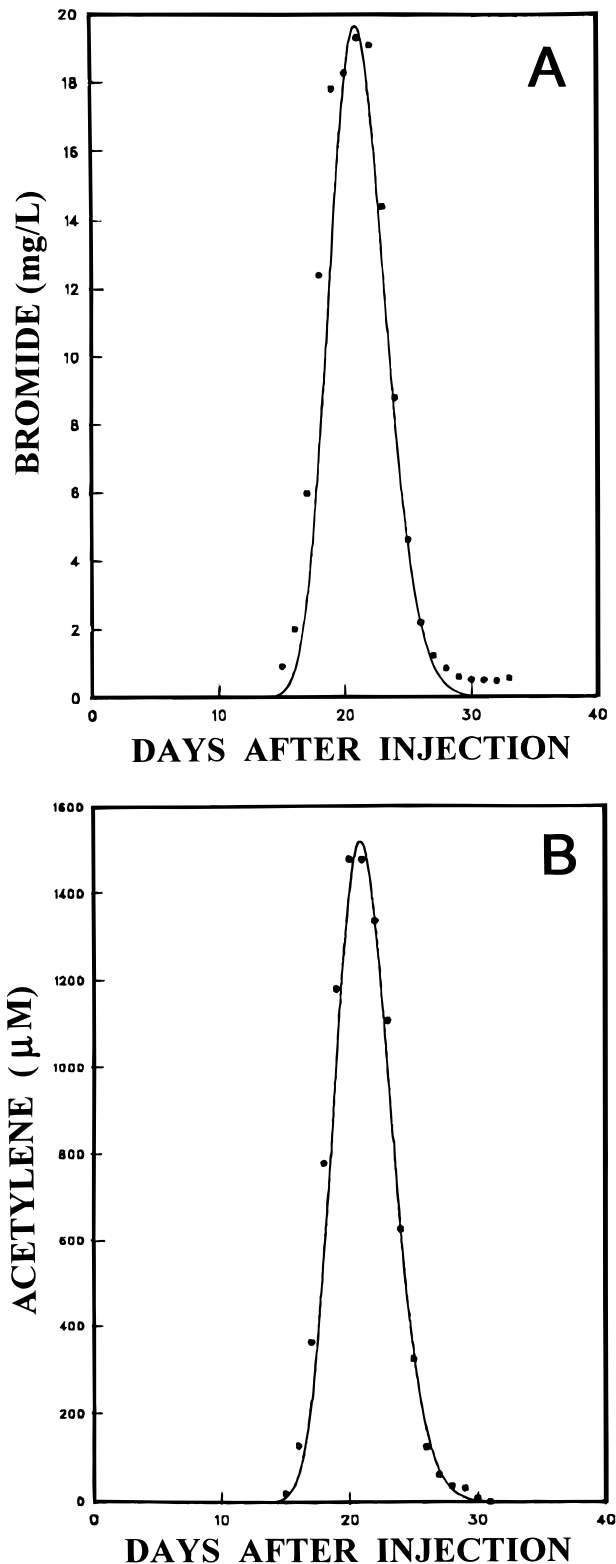


FIGURE 6. Simulated (lines) and observed (data points) breakthrough curves of (A) bromide and (B) acetylene for the 1991 acetylene block tracer test. Values used for model parameters were  $\alpha_L = 0.05$  m,  $v = 0.45$  m/d.

increase of ~30 μM above ambient concentrations was evident after 10 m of transport (Figure 5). Acetylene was transported conservatively; breakthrough curves normalized to the injectate concentration were virtually identical to those of bromide. Nitrous oxide breakthrough curves peaked 2–3 days after and were 6–7 days narrower than the acetylene and bromide curves (Figure 5). The later

TABLE 2

## Parameter Values for Model Simulations

tracer test	figure	solute	velocity (m/d)	dispersivity (m)	N <sub>2</sub> O rate <sup>a</sup> (nmol cm <sup>-3</sup> day <sup>-1</sup> )	A <sub>min</sub> (μM)	A <sub>max</sub> (μM)	time lag (d)
1991	6A	Br	0.45	0.05				
1991	6B	C <sub>2</sub> H <sub>2</sub>	0.45	0.05				
1991	7A	N <sub>2</sub> O	0.45	0.05	0.39	0	10	0
1991	7A	N <sub>2</sub> O	0.45	0.05	0.59	0	10	0
1991	7A	N <sub>2</sub> O	0.45	0.05	0.78	0	10	0
1991	7B	N <sub>2</sub> O	0.45	0.05	0.59	50	51	0
1991	7B	N <sub>2</sub> O	0.45	0.05	0.59	500	501	0
1991	7B	N <sub>2</sub> O	0.45	0.05	0.59	1000	1001	0
1991	7C	N <sub>2</sub> O	0.45	0.05	0.59	1	10	0
1991	7C	N <sub>2</sub> O	0.45	0.05	0.59	1	10	2
1991	7C	N <sub>2</sub> O	0.45	0.05	0.59	1	10	4
<b>Best Fit Simulations</b>								
1991	8A	N <sub>2</sub> O	0.45	0.05	1.51	500	501	4
1992	8B	N <sub>2</sub> O	0.37	0.05	0.60	500	501	4

<sup>a</sup> Production rates were calculated assuming an aquifer porosity of 0.39 (17).

arrival of the nitrous oxide peak was due to continued effectiveness of the acetylene block at less than peak acetylene concentrations, and thus continued accumulation of nitrous oxide in the trailing portions of the tracer cloud. Nearly identical results were obtained in replicate tracer tests in successive years (Figure 5). The main difference between the tests (the travel time) was due to a change in groundwater velocity, which was likely caused by a shift in the slope of the water table. Consequently, the tracer clouds for the two tests were transported along different flow paths and arrived at different MLSs in the 10 m row of sampling wells. Groundwater nitrate concentrations were unaffected by the tracer clouds and remained constant during the acetylene and nitrous oxide breakthrough curves (data not shown), though there were regional fluctuations in trace constituents, such as nitrous oxide, which were not related to the tracer test (e.g., see Figure 5B).

Rates of denitrifying activity within the tracer test transport interval were determined using an interpretive numerical model (eq 4) to simulate the effect of advection and dispersion upon both the acetylene and bromide tracers and the nitrous oxide produced. The transit time of the tracer cloud was very short relative to the amount of nitrate consumed, thus the electron-donor and electron-acceptor concentrations were essentially constant for the duration of the tracer test. This reduced the complexity needed for the model. Rates of denitrification were calculated using a zero-order reaction term because nitrate levels greatly exceeded saturation kinetics for the denitrification enzyme pathway. Using this approach, the model effectively simulated the breakthrough curves of both bromide and acetylene for the tracer experiments conducted in 1991 (Figure 6) and 1992 (data not shown). The groundwater velocities ( $v$ ) and dispersivities ( $\alpha_L$ ) were calibrated by fitting the bromide breakthrough curves with  $k_{max}$  set to zero. The groundwater flow velocities in the best fit simulations were 0.45 and 0.37 m/day in 1991 and 1992, respectively (Table 2). A single value was used for dispersivity, 0.05 m; the model simulations were not very sensitive to changes in dispersivity.

Then, using the calibrated values for  $v$  and  $\alpha_L$ , the nitrous oxide production rate ( $k_{max}$ ) was determined by adjusting its value to match the model predictions to the peak nitrous oxide breakthrough curve (Figure 7A, Table 2). The values of  $k_{max}$  were calculated assuming a constant porosity (0.39) for all the simulations. This assumption appears reasonable

given that the aquifer porosity was found to be constant in a tracer test conducted at this site with a much larger travel distance (11). In the simulations shown in Figure 7A, the threshold level for the acetylene block was kept low ( $A_{min} = 0.0 \mu\text{M}$ ;  $A_{max} = 10 \mu\text{M}$ ). These values were chosen based on the sensitivity of nitrous oxide consumption by surface soils to various acetylene concentrations (21). Using the zero-order production term, the model could effectively simulate the arrival time of the nitrous oxide peak, 2 days after the acetylene and bromide peaks. However, the nitrous oxide breakthrough curve in these simulations is too broad. That is, too much nitrous oxide is produced during the early and later periods of the simulated breakthrough curves in comparison to measured nitrous oxide concentrations. This over production occurs irrespective of  $k_{max}$  values (Figure 7A), even for best-fit simulations ( $k_{max} = 0.59 \text{ nmol cm}^{-3} \text{ aquifer day}^{-1}$ ) that match the nitrous oxide peak concentration. Therefore, it was concluded that parameters other than  $k_{max}$  must also be calibrated in order to fit the observed nitrous oxide breakthrough curve.

Increasing the model threshold level of acetylene required to produce an effective block ( $A_{min}$ ) results in less nitrous oxide production and a narrowing of the simulated breakthrough curves. Changes in  $A_{min}$  from 0 to 1000  $\mu\text{M}$  at a constant  $k_{max}$  ( $0.59 \text{ nmol cm}^{-3} \text{ aquifer day}^{-1}$ ) are shown in Figure 7 A,B. For these simulations,  $A_{max}$  values are kept close to  $A_{min}$  values (Table 2), in essence creating a step function; the model is much more sensitive to changes in  $A_{min}$  than  $A_{max}$ . However, the highest acetylene threshold tested (1000  $\mu\text{M}$ ), which is probably unrealistic and greatly exceeds even the "extra" acetylene needed when nitrate concentrations are low (17), still results in a breakthrough curve that is too broad. In addition, as the acetylene threshold is increased, the simulated breakthrough curve moves toward earlier arrival, no longer matching the time of the measured peak nitrous oxide concentrations (Figure 7B).

Another mechanism that would narrow the nitrous oxide peak would be a time lag between exposure to acetylene and the subsequent inhibition of nitrous oxide reductase. As noted above, flask incubations with aquifer core material and acetylene commonly display a lag in nitrous oxide accumulation. Previously the lag has been viewed as resulting from sampling and flask effects (18), but it could also represent a fundamental delay in response to the acetylene by denitrifiers under the low biomass, nutrient-

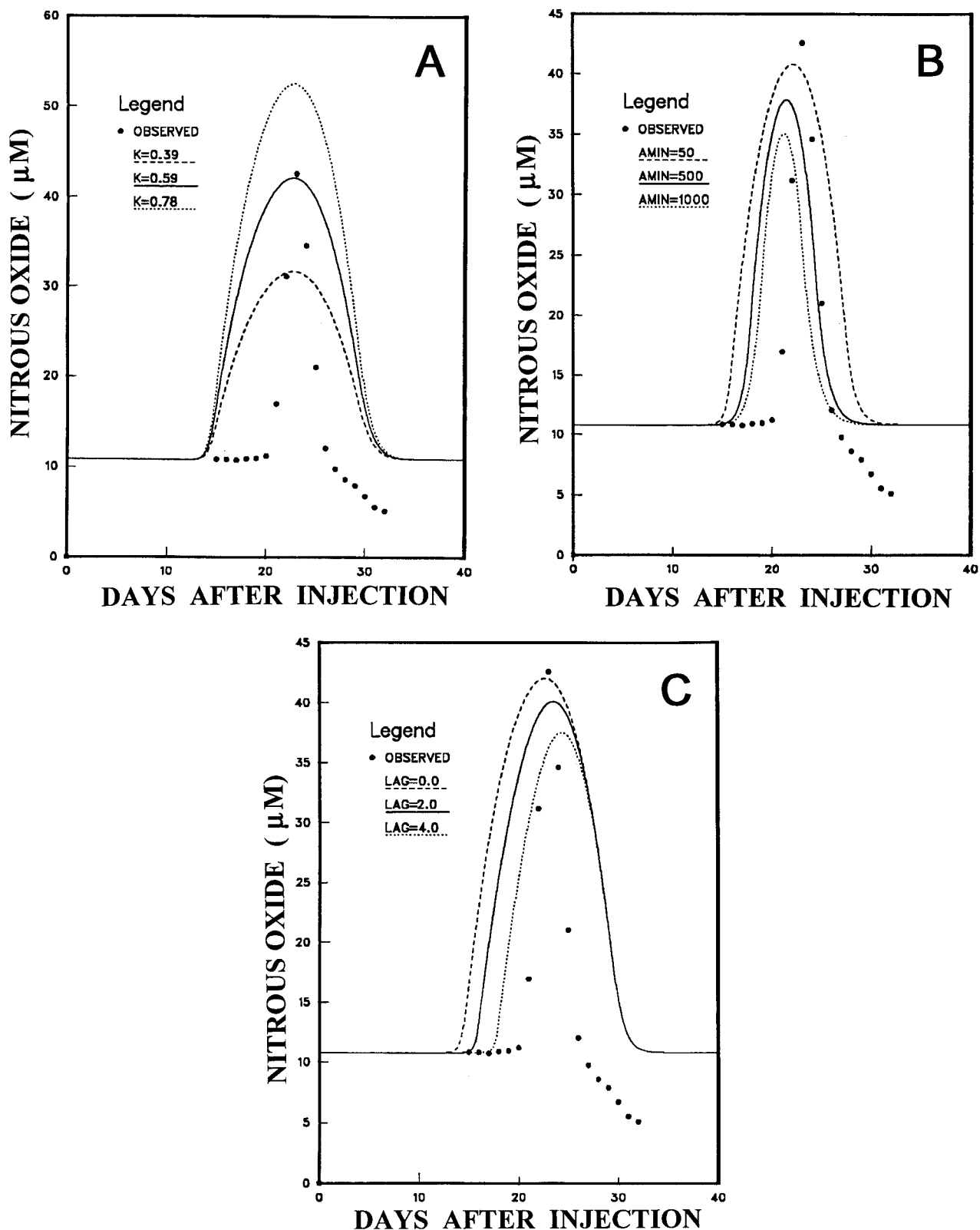


FIGURE 7. Simulated (lines) and observed (data points) breakthrough curves of nitrous oxide for the 1991 acetylene block tracer test. Shown is the sensitivity of the model simulations to changes in (A)  $\text{N}_2\text{O}$  production rate ( $k_{\text{max}}$ ,  $\text{nmol cm}^{-3} \text{day}^{-1}$ ), (B) acetylene threshold concentrations ( $A_{\text{min}}$  and  $A_{\text{max}}$ ,  $\mu\text{M}$ ), and (C) length of the time lag (days). Values used for the model parameters are given in Table 2.

and energy-poor conditions present in the aquifer. The effect of including a 0–4-day time delay in the model on nitrous oxide production after the acetylene concentration exceeds  $A_{\text{min}}$  is shown in Figure 7C. For a fixed nitrous oxide production rate, the peak becomes smaller and shifts toward a later arrival as the time lag increases. This shift in arrival time plays a critical role in the model simulations

because this effect counteracts the earlier arrival of the peak concentration caused by an increase in  $A_{\text{min}}$ .

Combining the calibration values of  $A_{\text{min}}$  (500  $\mu\text{M}$ ) and the time lag (4 days) produces a reasonable fit to the observed nitrous oxide breakthrough curve (Figure 8A), with an increase in  $k_{\text{max}}$  to 1.51  $\text{nmol cm}^{-3} \text{aquifer day}^{-1}$  to match the observed peak concentration. The model was also able

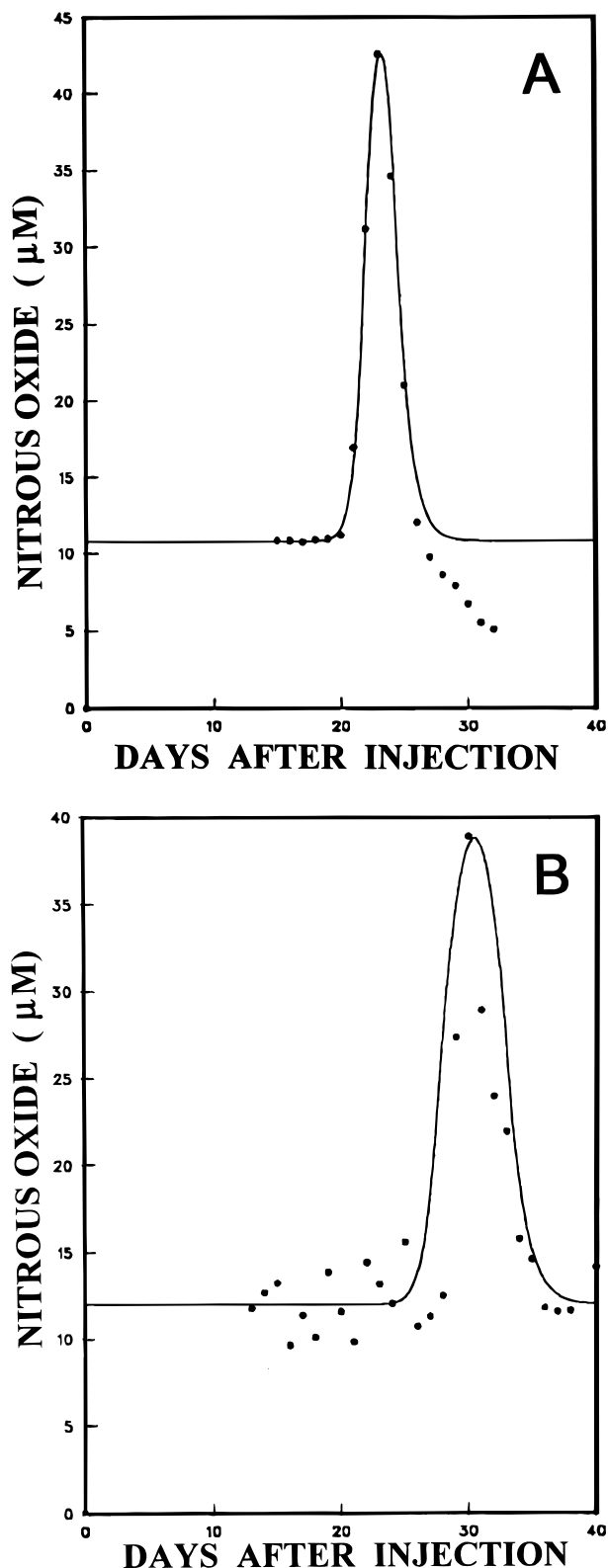


FIGURE 8. Best-fit simulated (lines) breakthrough curves and observed nitrous oxide concentrations (data points) for (A) 1991 and (B) 1992 tracer tests. Values used for the model parameters are given in Table 2.

to simulate the 1992 experiment very well by using the same  $A_{\min}$  and time lag values and only adjusting the groundwater flow velocity to account for the earlier arrival of the acetylene and bromide, and the  $k_{\max}$  (Figure 8B, Table 2). Therefore, the in situ estimate of denitrification in this portion of the aquifer was in the range of 0.60–1.51 nmol

TABLE 3

### Comparison of Denitrification Rate Estimates

technique	$N_2O$ production (nmol $cm^{-3}$ aquifer $day^{-1}$ )
sediment slurry incubation	1.85–4.32 <sup>a</sup>
intact core incubation	
0-day lag	2.43–7.75 <sup>b</sup>
4-day lag	4.86–15.5 <sup>b</sup>
tracer tests	0.60–1.51 <sup>c</sup>

<sup>a</sup> Range from three cores. <sup>b</sup> Range from six 0.3-m core segments, two each from three cores. For comparison, rates are calculated both with and without a 4-day time lag for the onset of nitrous oxide accumulation. The time lag has been factored into the results of the other two incubation techniques. <sup>c</sup> Rates from Table 2.

of  $N_2O$  produced  $cm^{-3}$  aquifer  $day^{-1}$ . The basic approach to calibrate the model was to change only single parameter values at one time and only to the degree necessary to match the observed curve. The model does not arrive at unique solutions for the time lag,  $A_{\min}$ , and  $k_{\max}$ . However, because  $A_{\min}$  and the time lag counteract each other, within reasonable limits, changes in one must be offset by changes in the other, and there is only a relatively small effect upon the rate of activity ( $k_{\max}$ ).

The combination tracer test model approach then suggests that the function of the acetylene block technique for groundwater denitrification is somewhat different than has been interpreted for pure cultures and soils. That difference, which is corroborated by the sediment slurry results, can be successfully simulated by incorporating a relatively low sensitivity and a delayed response to the presence of acetylene. It is unknown whether these are the actual mechanism(s) involved or whether some other factor manifests this result. The aquifer contains no detectable sulfide, which has been shown to reduce the effectiveness of the acetylene block technique (31, 32). However, the effect appears to be specific to acetylene. Using  $^{15}N$ -enriched nitrate as a tracer, breakthrough curves of  $^{15}N_2$  are similar in width and arrival time to those of bromide (R. L. Smith, unpublished data).

A comparison of the denitrification rate estimates between the in situ tracer test approach and the laboratory incubations is presented in Table 3. The units for each measurement have been converted to a unit volume of aquifer (groundwater plus solids) with a porosity of 0.39. The rates of activity for laboratory incubations with the core material are 1.2–13 times higher than the in situ rates (or up to 26-fold higher if the 4-day lag that appears to be appropriate for the sediment slurries and the tracer tests is also applied to the intact core incubations). Though such a direct comparison has rarely, if ever, been made for groundwater, this is a result that might be expected. In surface water studies, alteration of natural rates of many types of microbial activities during laboratory incubations is well known as the "bottle effect". This effect is often a stimulation of activity if the sampling and incubation procedure involves enhanced mixing or delivery of nutrients (33, 34), which also usually occurs during collection and handling of subsurface core material. Microcosm experiments using radiolabeled substrates added to deep groundwater core material yielded rate measurements that were  $10^1$ – $10^6$  times higher than calculations based upon geochemical models and changes in groundwater chemistry along inferred groundwater flow paths (3, 4). Obviously, interpretation of a nonlinear time course from an activity measurement (e.g., Figure 4) can be difficult and could

result in a wide range of potential rate estimates for a single sample. On the other hand, static, intact core incubations usually do not provide information regarding changes in response as a function of time, and they exclude the dynamics of the flowing porewater. Natural-gradient tracer tests can conduct the same activity measurement in situ, eliminate the disturbance factor associated with coring, minimally alter the hydrology of and the geochemical gradients within an aquifer, and can be conducted using substrates enriched with stable isotopes as tracers (5).

A potential factor contributing to the range in rate estimates between and among cores (Figure 4, Table 1) is small-scale heterogeneity. Heterogeneity can be present in aquifer composition and physical properties as well as in the distribution of microbial populations and activities. Hess et al. (13) determined that spatial correlation scales of hydraulic conductivity ( $K$ ) in the relatively uniform Cape Cod aquifer were 2.9–8.0 and 0.18–0.38 m on horizontal and vertical axes, respectively. The tracer test sites are more aligned with this spatial orientation than are the 5 cm diameter (horizontal), 1.5 m long (vertical) cores. Adrian et al. (35) determined the in situ spatial variability of methane production in a landfill-contaminated sandy aquifer. They found that at two sites the coefficients of variation were 340 and 490% of the mean and that anaerobic biodegradation rates were distributed log-normally rather than normally. Other studies have demonstrated changes in microbial biomass and activity measurements across vertical gradients that can be very steep (36, 37). In particular, denitrification is a process that is typically characterized by patchy distribution, especially in soils (38, 39). During natural-gradient tests in groundwater, the tracer cloud is subjected to whatever heterogeneity occurs along a flow path. The result is an integrated activity measurement, equivalent to collecting several hundred cores for laboratory incubations. Thus, beside representing an in situ determination with minimal disturbance, the tracer test results have applicability on a larger scale because they factor small-scale variability into the rate estimate.

In summary, natural-gradient tracer tests using acetylene in a nitrate-contaminated, unconfined aquifer demonstrated in situ denitrifying activity. The rate of nitrous oxide production could be calculated by applying a one-dimensional transport model that accounts for advection, dispersion, and a zero-order production term to tracer cloud breakthrough curves. The model suggested that denitrification within the aquifer may have a reduced sensitivity to acetylene. Rates of activity in core material collected in conjunction with the tracer tests were up to 13 times higher and quite variable. This over-estimation by laboratory activity assays must be viewed as a limitation for extrapolating such results to the field, especially for predictive purposes.

## Acknowledgments

We thank D. R. LeBlanc, coordinator of the Cape Cod site, for field and technical assistance, and J. K. Bohlke, T. Yoshinari, and L. DeSimone for manuscript reviews. This study was funded by the U.S. Geological Survey Toxic Substances Hydrology Program. The use of trade or product names in this paper is for identification purposes only and does not constitute endorsement by the U.S. Geological Survey.

## Literature Cited

(1) Ghiorse, W. C.; Wilson, J. T. *Adv. Appl. Microbiol.* **1988**, *33*, 107.

- (2) Chapelle, F. H. *Ground-Water Microbiology and Geochemistry*; John Wiley & Sons, Inc.: New York, 1993.
- (3) Chapelle, F. H.; Lovley, D. R. *Appl. Environ. Microbiol.* **1990**, *56*, 1865.
- (4) Phelps, T. J.; Murphy, E. M.; Pfiffner, S. M.; White, D. C. *Microb. Ecol.* **1994**, *28*, 335.
- (5) Smith, R. L.; Howes, B. L.; Garabedian, S. P. *Appl. Environ. Microbiol.* **1991**, *57*, 1997.
- (6) Harvey, R. W.; George, L. H.; Smith, R. L.; LeBlanc, D. R. *Environ. Sci. Technol.* **1989**, *23*, 51.
- (7) LeBlanc, D. R. *U.S. Geol. Surv. Water-Supply Pap.* **1984**, No. 2218.
- (8) Ceazan, M. L.; Thurman, E. M.; Smith, R. L. *Environ. Sci. Technol.* **1989**, *23*, 1402.
- (9) Harvey, R. W.; Garabedian, S. P. *Environ. Sci. Technol.* **1991**, *25*, 178.
- (10) Kent, D. B.; Davis, J. A.; Anderson, L. C. D.; Rea, B. A.; Waite, T. D. *Water Resour. Res.* **1994**, *30*, 1099.
- (11) LeBlanc, D. R.; Garabedian, S. P.; Hess, K. M.; et al. *Water Resour. Res.* **1991**, *27*, 895.
- (12) Garabedian, S. P.; LeBlanc, D. R.; Gelhar, L. W.; Celia, M. A. *Water Resour. Res.* **1991**, *27*, 911.
- (13) Hess, K. M.; Wolf, S. H.; Celia, M. A. *Water Resour. Res.* **1992**, *28*, 2011.
- (14) Smith, R. L.; Howes, B. L.; Duff, J. H. *Geochim. Cosmochim. Acta* **1991**, *55*, 1815.
- (15) Barber, L. B., II; Thurman, E. M.; Schroeder, M. P.; LeBlanc, D. R. *Environ. Sci. Technol.* **1988**, *22*, 205.
- (16) Harvey, R. W.; Barber, L. B., II *J. Contam. Hydrol.* **1992**, *9*, 91.
- (17) Smith, R. L.; Duff, J. H. *Appl. Environ. Microbiol.* **1988**, *54*, 1071.
- (18) Brooks, M. H.; Smith, R. L.; Macalady, D. L. *Appl. Environ. Microbiol.* **1992**, *58*, 1746.
- (19) Smith, R. L.; Ceazan, M. L.; Brooks, M. H. *Appl. Environ. Microbiol.* **1994**, *60*, 1949.
- (20) Zapico, M. M.; Vales, S.; Cherry, J. A. *Ground Water Monit. Rev.* **1987**, *7*, 74.
- (21) Yoshinari, T.; Hynes, R.; Knowles, R. *Soil Biol. Biochem.* **1977**, *9*, 177.
- (22) Huyakorn, P. S.; Pinder, G. F. *Computational Methods in Subsurface Flow*; Academic Press: New York, 1983.
- (23) Smith, R. L.; Miller, L. G.; Howes, B. L. *Biogeochemistry* **1993**, *21*, 95.
- (24) Weiss, R. F.; Price, B. A. *Mar. Chem.* **1980**, *8*, 347.
- (25) Miller, S. A. *Acetylene: Its Properties, Manufacture and Uses*; Academic Press: New York, 1965; Vol. 1, p 74.
- (26) Fishman, M. J.; Friedman, L. C. *Open-File Rep.—U.S. Geol. Surv.* **1985**, No. 85–495.
- (27) Fishman, M. J.; Schroder, L. J.; Friedman, L. C.; Arozarena, C. E.; Hedley, A.G. *Water Res.* **1985**, *19*, 497.
- (28) Smith, R. L.; Harvey, R. W.; LeBlanc, D. R. *J. Contam. Hydrol.* **1991**, *7*, 285.
- (29) DeSimone, L. A.; Howes, B. L. *Environ. Sci. Technol.* **1996**, *30*, 1152.
- (30) Jorgensen, B. B. *Geomicrobiol. J.* **1978**, *1*, 29.
- (31) Jensen, K. M.; Cox, R. P. *FEMS Microbiol. Lett.* **1992**, *96*, 13.
- (32) Knowles, R. In *Denitrification in Soil and Sediment*; Revsbech, N. P., Sorensen, J., Eds.; Plenum Press: New York, 1990; p 151.
- (33) Dobbs, F. C.; Guckert, J. B.; Carman, K. R. *Microb. Ecol.* **1989**, *17*, 237.
- (34) Findlay, R. H.; Pollard, P. C.; Moriarty, D. J. W.; White, D. C. *Can. J. Microbiol.* **1985**, *31*, 493.
- (35) Adrian, N. R.; Robinson, J. A.; Sufliata, J. M. *Appl. Environ. Microbiol.* **1994**, *60*, 3632.
- (36) Federle, T. W.; Ventullo, Roy M.; White, D. C. *Microb. Ecol.* **1990**, *20*, 297.
- (37) Keeley, J. E. In *Stable Isotopes in Ecological Research*; Rundel, P. W., Ehleringer, J. R., Nagy, K. A., Eds.; Springer-Verlag: New York, 1989; p 76.
- (38) Christensen, S.; Simkins, S.; Tiedje, J. M. *Soil Sci. Soc. Am. J.* **1990**, *54*, 1608.
- (39) Parkin, T. B. In *Denitrification in Soil and Sediment*; Revsbech, N. P., Sorensen, J., Eds.; Plenum Press: New York, 1990; p 213.

Received for review January 17, 1996. Revised manuscript received July 17, 1996. Accepted July 26, 1996.®

ES960042G

® Abstract published in *Advance ACS Abstracts*, October 15, 1996.